energies

Article

Day-Ahead Optimization of Proton Exchange Membrane Electrolyzer Operations Considering System Efficiency and Green Hydrogen Production Constraints Imposed by the European Regulatory Framework

Giuseppe Graber [1,*], Vito Calderaro [1], Vincenzo Galdi [1], Lucio Ippolito [1], Fabrizio De Caro [1] and Alfredo Vaccaro [2]

[1] Department of Industrial Engineering, University of Salerno, Via Giovanni Paolo II, 132, 84084 Fisciano, SA, Italy; vcalderaro@unisa.it (V.C.); vgaldi@unisa.it (V.G.); ippolito@unisa.it (L.I.); fadecaro@unisa.it (F.D.C.)

[2] Department of Engineering, University of Sannio, Via Roma, 21, 82100 Benevento, BN, Italy; vaccaro@unisannio.it

* Correspondence: ggraber@unisa.it; Tel.: +39-089-96-4290

Abstract: Clean hydrogen (H_2) use (i.e., produced using either renewable or low-carbon energy sources) can help decarbonize energy-intensive industries, the transport sector, and the power sector. The European regulatory framework establishes that the production of green H_2 must be supported either by the electricity grid through a power purchase agreement (PPA) or by intermittent renewable energy source (RES) plants owned by the hydrogen producer. Although the issue of the optimization of hydrogen production costs has already been approached, constraints related to the current regulatory framework and the modeling of nonlinear electrolyzer efficiency still represent open problems. In this paper, a mixed-integer linear programming (MILP) problem, assuming as the objective function the overall cost minimization of the allowed energy mix for green H_2 production, is formulated. Two approaches are compared: in the first one, electrolyzers can only operate at 100% load, whereas the second one allows for more flexible electrolyzer scheduling, by enabling partial-load working operations. The simulation results of several scenarios considering different H_2 production targets, forecasted RES production, and cost for PPAs demonstrate the effectiveness of the proposed methodology.

Keywords: cost optimization; PEM electrolyzer; green hydrogen; optimization; scheduling strategy

check for updates

Citation: Graber, G.; Calderaro, V.; Galdi, V.; Ippolito, L.; De Caro, F.; Vaccaro, A. Day-Ahead Optimization of Proton Exchange Membrane Electrolyzer Operations Considering System Efficiency and Green Hydrogen Production Constraints Imposed by the European Regulatory Framework. *Energies* **2024**, *17*, 5713. https://doi.org/10.3390/en17225713

Academic Editor: Massimo Guarnieri

Received: 11 October 2024
Revised: 4 November 2024
Accepted: 12 November 2024
Published: 15 November 2024

Copyright: © 2024 by the authors. Licensee MDPI, Basel, Switzerland. This article is an open access article distributed under the terms and conditions of the Creative Commons Attribution (CC BY) license (https://creativecommons.org/licenses/by/4.0/).

1. Introduction

In 2023, the European Commission formally published two delegated acts outlining detailed rules on the EU definition of green hydrogen (H_2) specifically produced with excess photovoltaic (PV) and wind power. Therefore, the role of power-to-hydrogen ($P2H_2$) becomes paramount for increasing the share of renewable energy in the power sector. Indeed, $P2H_2$ can provide grid-balancing services and long-term storage to manage the variability in power supply from intermittent renewable energy sources (RESs). Moreover, $P2H_2$ enables the use of green H_2 to decarbonize transport, industry, and other sectors [1]. With the increasing penetration of RESs, large-scale storage solutions and grid stability management are becoming critical issues in system operation. Electrolyzers can help integrate RESs into power systems, as their electricity demand can be adjusted to follow wind and PV power generation, thereby providing grid-balancing services [1,2]. Procuring excess renewable energy (which is likely to be curtailed or sold at near-zero marginal prices) can significantly help improve the economics of hydrogen production. The offtake of excess renewable energy also enables RES asset owners to gain incremental revenues and reduces their exposure to volatility in power prices [1,2].

However, the European regulatory framework, with the Renewable Energy Directive (RED) III and the Delegated Regulation on Additionality (DRA), establishes that the production of green hydrogen must be supported either by the electricity grid through a power purchase agreement (PPA) or by RES plants owned by the hydrogen producer [3]. In more detail, the DRA limits the energy that can be purchased from the grid to produce a given quantity of green H_2. Electricity taken from the grid may be recognized as fully renewable only if it meets the criteria of additionality, geographical correlation, and temporal correlation [4].

1.1. Bibliographic Survey and Research Gap

In the technical literature, green H_2 production cost optimization is a widely addressed problem. Specifically, several economic analyses have been implemented: in [5], the assessment of Morocco's potential for green H_2 generation from RES is investigated, whereas the payback period of a green H_2 plant comprising PV and wind power plants, battery storage units, and a 1 MW proton exchange membrane (PEM) electrolyzer is reported in [6]. A novel and effective approach for calculating the levelized cost of hydrogen production across the globe is proposed in [7]. Representative patterns of RES production are applied to evaluate the proportion of electricity that electrolyzers can use. A long-term planner for daily H_2 production is proposed in [8], where historical data and short-term forecasts address the impracticality of full foresight assumption, which often leads to the underestimation of both costs and CO_2 emissions.

The study in [9] examines the potential for H_2 production of the Shagaya renewable power plant. Techno-economic and optimization analyses are used to reduce costs while increasing the RES fraction and lowering CO_2 emissions. The GeoH_2 model, introduced in [10], optimizes the production and transport costs of green H_2 in a specified location to meet the demands in another location. Economic aspects drive the development of electrolysis in industrial clusters; the study in [11] focuses on the trade-off between hydrogen and electricity infrastructure. Specifically, it shows that, in a configuration with delocalized renewable electricity production, transporting hydrogen via a pipeline is cheaper than transporting the electrical equivalent energy and producing the hydrogen at the demand site, for distances below 150 km.

The capacity allocation optimization of a combined pumped storage and H_2 production system based on wind and PV generation is presented in [12], aiming to reduce green H_2 production costs. Hydrogen energy storage plays crucial roles in enhancing the consumption of renewable energy, reducing energy loss, and improving comprehensive energy utilization rates. The study in [13] proposes a joint topology and configuration optimization method to address these challenges and minimize the overall costs. A bi-level strategic operation model for hydrogen energy service providers is proposed in [14]. In the first level, H_2 production and transportation are coordinated to minimize the overall costs, whereas, in the other one, market clearing is simulated to estimate the influence of H_2 production on electricity prices.

In [15], a novel mathematical programming formulation is developed for the simultaneous optimal design and operation of standalone green H_2 production systems, identifying shortcomings in the design stage which can lead to expensive operational conditions. In [16], based on the time-sequence production simulation method, a two-stage optimal proportion model for an integrated system of wind–solar–hydrogen–storage is formulated, calculating the optimal capacity of each generation equipment in the system. An expected operational cost minimization problem for green H_2 production is approached in [17], considering nonlinear characteristics. Specifically, an online operation algorithm minimizes the total operational cost based on proximal policy optimization and expert knowledge.

An optimization model for multi-energy system operation is presented in [18], including the characteristics of the P2H_2 devices, whereas, in [19], a bi-level optimal programming model for the configuration of the capacity of the P2H_2 facilities is derived to achieve the maximum benefits of wind power plants. A long-duration robust optimization framework

for integrated P2H_2 systems, considering energy, ancillary services, and hydrogen markets, is proposed in [20]. A unified capacity-bidding model in the ancillary service market is established for fuel cells and electrolyzers to simulate the bidding strategy in typical markets. Moreover, green H_2 production through electrolyzers using electrical energy from solar PV and electricity generation using PEM fuel cells are investigated in [21] to supply residences and electric vehicles. In [22], the economic efficiency and optimization of a PV grid-connected system for green H_2 production are discussed, where the produced hydrogen is used for refueling fuel cell vehicles or stationary applications.

Optimization models aimed at using electrolyzers for grid support through H_2 production are approached in [23–26]. In [23], coordinated operation scheduling of a renewables–hydrogen system with multi-electrolyzers is investigated, and a refined rolling optimization strategy is developed, considering technical, economic, and environmental benefits, to comprehensively improve green H_2 production. The integration of an electrolyzer fleet to reduce overvoltage events and voltage fluctuations is investigated in [24], whereas cost-competitive participation in ancillary service markets for offshore wind-based hydrogen production is proposed in [25]. Finally, the optimization of electrolyzer efficiency to reduce H_2 production costs is approached in [26], where performance optimization is evaluated by selecting appropriate operating conditions.

Although the electrolyzer cost optimization problem has been approached from both the technical and economic point of view, the above literature review reveals several research gaps: for instance, constraints related to the current regulatory framework are neglected, despite their significant impact on green H_2 production costs [27,28]. Moreover, existing operation optimization methods do not consider the nonlinear characteristics of electrolyzers and fuel cells, resulting in significant errors in the effective estimation of H_2 production throughout the day [28,29]. Indeed, electrolyzers' efficiency behavior in high-load zones shows an increasing trend as the load decreases, as noted in [30]. Finally, in most papers, the amount of H_2 that must be produced during the day is often not defined a priori. Thus, the H_2 production target is not imposed as a constraint, which represents an important aspect for hydrogen producer's business, because the daily production target significantly impacts the H_2 costs by defining electrical resources which must be bought or produced to meet the contracted demand.

1.2. Proposal and Main Contribution

Here, a day-ahead methodology for scheduling electrolyzer operations near wind and/or PV power plants has been formulated as a mixed-integer linear programming (MILP) problem. The aim is to minimize the cost of electrical energy to obtain an a priori defined daily target for green H_2 production. Specifically, the proposed strategy considers a mix of excess renewable energy, hourly electricity prices, and the cost for PPAs to identify the most economically advantageous time intervals during the day when electrolyzers must operate, in accordance with EU regulations which limit the amount of energy acquired by the sources of the above mix. Moreover, the electrolyzer efficiency curve is considered to assess the impact of the ON/OFF at full load and the partial-load operating strategy of the electrolyzer on the green H_2 production cost.

Therefore, the original contributions of this paper can be summarized in the following three points:

- Defining a novel mathematical formulation for the production cost optimization problem of green H_2, taking EU regulatory aspects into account as constraints;
- Modeling electrolyzer efficiency and proposing a methodology to include it, while maintaining day-ahead cost optimization as an MILP problem;
- Developing an extensive simulation framework that includes daily H_2 production as a target for defining the energy resource mix and estimating the green H_2 cost per kg, comparing it to that of gray and blue H_2.

Section 2 describes electrolysis technologies and the current EU regulations, while Section 3 formulates the cost optimization problem. Finally, several scenarios are analyzed,

considering different green H_2 production targets, RES generation, and the cost of PPAs, presented in Section 4. Concluding remarks will end this paper.

2. Green Hydrogen Production

Green hydrogen can be produced using electricity to split water into hydrogen and oxygen through electrolysis, which is an emission-free process. Currently, several types of water electrolysis technologies are available. However, the DRA establishes limits on the energy mix required to produce green hydrogen.

2.1. Technologies for Electrolyzer Units

To provide a more comprehensive overview of the production costs of green H_2, a summary of existing technologies is reported. Currently, there are various water electrolysis technologies. The main ones are (1) alkaline, (2) anion exchange membrane (AEM), (3) PEM, and (4) solid oxide. A technological comparison is reported in [31].

Alkaline electrolyzers are a well-established, mature technology for industrial hydrogen production up to the megawatt range, with commercial applications. Alkaline water electrolysis is a favorable system design for large-scale applications. Currently, investment costs for alkaline water electrolysis range from 500 to 1000 USD/kW, and the system's lifetime is about 90,000 h. The major challenges associated with alkaline electrolyzers include limited current densities (0.1–0.5 A/cm^2) and the use of corrosive electrolytes [31–33].

To overcome the drawbacks of alkaline water electrolysis, PEM technology was developed [34]. PEM water electrolysis is safer than alkaline water electrolysis due to the absence of caustic electrolytes and its smaller footprint. As a result, several manufacturers are currently developing large-scale (up to MW) PEM electrolyzers for industrial and transportation applications. The reported stability of PEM electrolyzers is 60,000 h, with a negligible loss of performance. Compared to alkaline electrolyzers, PEM electrolyzers operate at lower temperatures (30–80 °C), with higher current densities (1–2 A/cm^2), and produce high-purity (99.999%) hydrogen and oxygen gasses. However, the major challenge associated with PEM electrolyzers is the high cost of the components [31–33].

Several technologies are still under development, promising interesting advancements [35]. AEM technologies are like conventional alkaline technologies, with the main difference being the replacement of conventional diaphragms with an anion exchange membrane. AEM water electrolysis offers several advantages, the most notable being the use of cost-effective transition metal catalysts instead of noble metal catalysts. Currently, several research organizations and institutions are actively working on the development of AEM technologies up to the kW scale. The major challenges include the limited stability (at present, 35,000 h) and high hydrogen production costs [32,33].

At present, the technology of solid oxide water electrolysis is still in its development stage. Solid oxide water electrolyzers typically operate with water in the form of steam at high temperatures (500–850 °C), which can significantly reduce the power needed to split the water into H_2 and oxygen, thereby increasing the energy efficiency [36]. This improvement can lead to a significant reduction in electric energy consumption, as it is the main contributor to the H_2 production cost in electrolysis. Moreover, solid oxide water electrolysis does not require the use of noble metal electrocatalysts. Despite these advantages, insufficient long-term stability has prevented the commercialization of solid oxide electrolyzers. As of now, the reported stability is only 20,000 h [31–33].

Alkaline and PEM technologies are the most mature. However, according to Figures 1 and 2, PEM technologies are the best-performing. With the push towards zero-emission transportation, driven by both government policy and consumer demand, the market for H_2-powered solutions is projected to grow significantly in the coming years. Specifically, the market for PEM technologies in transportation is set to grow at a CAGR of 28% between 2024 and 2034 [37]. For this reason, PEM technology-based electrolyzers will be considered in this paper.

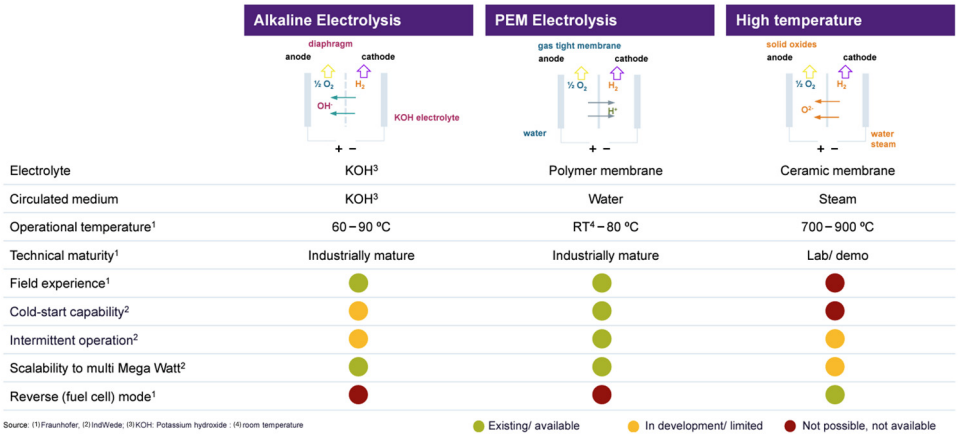


Figure 1. Comparison between technologies for water electrolysis [38].

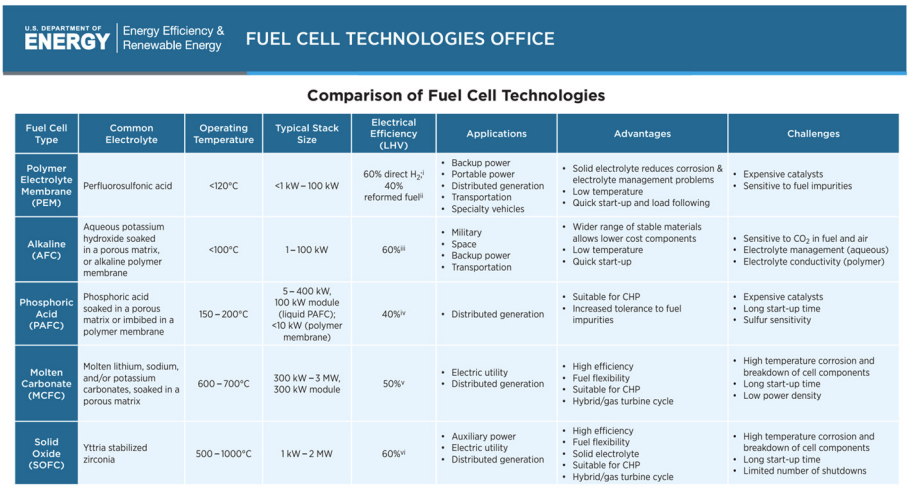


Figure 2. Comparison of fuel cell technologies [39].

Figure 3 shows turn-on and turn-off times of an MW-sized commercial PEM electrolyzer [30]. It can be observed that the turn-on phase, which includes a cold start, requires about one minute to rise from minimum load to full power. Afterward, it can match H_2 production to RES production by adjusting the load from a minimum of 5% to a maximum of 100%, with a dynamic response estimated at 10% per second. Therefore, ramp-up and ramp-down constraints do not appear to be necessary for the purpose of this paper, as the day-ahead scheduling is on an hourly basis.

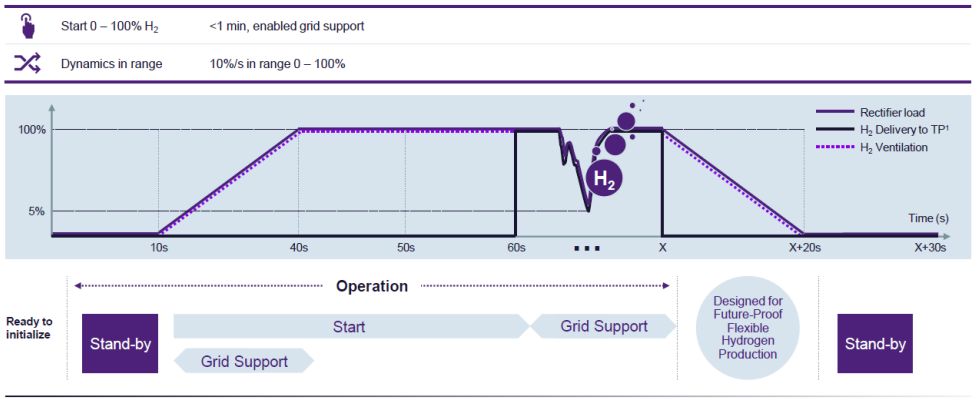


Figure 3. Siemens Energy—Silyzer 300 PEM electrolyzer dynamics [30].

On the other hand, Figure 4 shows the system efficiency curve according to the load of an MW-sized commercial PEM electrolyzer [40]. It can be observed that, as the load increases, the efficiency starts at a very low value and rises rapidly to its maximum. However, from about 40% of the maximum load to full power, the efficiency curve decreases from the peak value until it reaches the nominal value. This behavior is obtained by combining the auxiliary system efficiency curve with the DC efficiency curve (i.e., the efficiency of the PEM stack alone). In Section 3.2, a methodology for modeling the electrolyzer efficiency curve within an MILP problem is introduced.

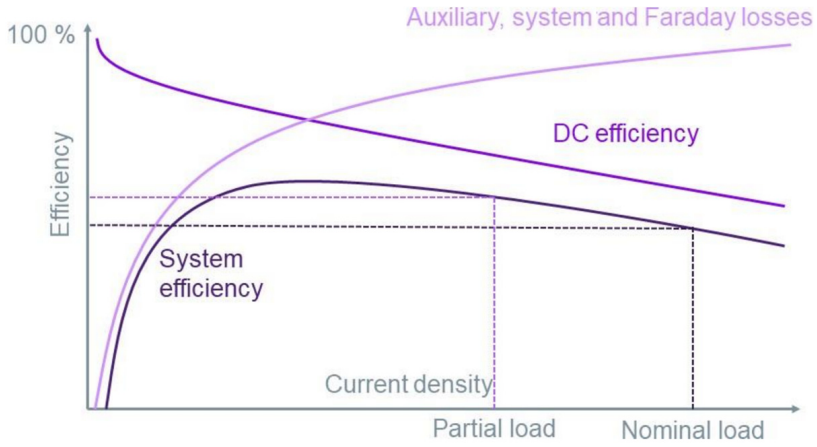


Figure 4. PEM electrolyzer efficiency according to the load [40].

2.2. European Regulatory Framework

Under the European Green Deal, renewable energy represents a pillar of clean energy transition. It is low-cost and home-grown, which reduces Europe's dependency on external suppliers. This is why the EU is focused on increasing the share of renewables in its energy mix, with the necessary measures being regularly revisited. Indeed, the RED EU/2018/2001 was revised in 2023, and the amending Directive EU/2023/2413 entered into force in November 2023 [3]. It sets an overall renewable energy target of at least 42.5% at the EU level by 2030. To support this uptake of renewables, the revised directive converts into EU law some of the concepts outlined in the directive regarding energy system integration and H_2 strategies published in 2020 [3]. In February 2023, the European Commission adopted two delegated acts related to the production and certification of renewable hydrogen. In particular, the DRA establishes the rules for producing green H_2.

In detail, the EU's regulatory approach defines the allowable energy mix, rather than a limit on CO_2 emissions from electricity generation, as the measure for considering the produced hydrogen to be green. As specified in RED II, electricity counts as being renewable if the renewable power plant and the electrolyzer are located in the same installation, or if there is a direct connection between them, and if electricity from the grid is not used for electrolysis. However, electricity taken from the grid may be recognized as fully renewable if it meets the criteria of additionality, geographical correlation, and temporal correlation [4].

Additionality indicates that hydrogen producers must ensure that the electricity used to produce hydrogen is matched by the production of renewable electricity in one of the following ways:

- In the same installation, demonstrating that the producers generate renewable electricity corresponding to the amount of hydrogen they claim as being renewable;
- Through a renewable power purchase agreement (PPA) with operators producing renewable electricity.

Geographical correlation highlights the fact that hydrogen producers must ensure that additional renewables are located within the area where hydrogen is being produced. At least one of the criteria listed below must be met regarding the location of the renewable electricity generator relative to the electrolyzer:

- In the same bidding zone as the electrolyzer;
- In an interconnected bidding zone with electricity prices in the day-ahead market equal to or higher than the bidding zone where the hydrogen is produced;
- In an offshore zone interconnected to the electrolyzer bidding zone.

Temporal correlation indicates that hydrogen producers must ensure that renewable electricity generation and H_2 production coincide temporally:

- Until 31 December 2029, hydrogen must be produced in the same calendar month as the renewable electricity produced under the PPA or from renewable electricity from a new storage asset directly connected to either the renewable electricity generator or the electrolyzer, charged in the same calendar month;
- From 1 January 2030, hydrogen must be produced during the same one-hour period as the renewable electricity or from renewable electricity from a co-located new storage asset that has been charged during the same one-hour period during which the electricity under the PPA was being produced.

However, under the DRA, there are several cases in which the criteria of additionality, temporal correlation, and geographical correlation need not be met. The most relevant case occurs when hydrogen production takes place in a bidding zone with an average renewable electricity share exceeding 90% in the previous calendar year [4]. In such cases, hydrogen may be counted as renewable if it does not exceed a maximum number of hours set in relation to the proportion of renewable electricity in the bidding zone. This maximum number of hours shall be calculated by multiplying the total number of hours in each calendar year by the share of renewable electricity reported for the bidding zone where H_2 is produced. The average share of renewable electricity shall be determined by dividing the gross final consumption of electricity from renewable sources in the bidding by the gross electricity production from all energy sources.

3. Green H_2 Production Cost Optimization

Here, the mathematical formulation of the proposed optimization problem aimed at scheduling the electrolyzer's daily operations is presented, along with a discussion on the linearization methodology for the nonlinear constraints related to the H_2 production target. It is worth noting that the proposed methodology can be extended to non-European regulatory frameworks and/or applied when existing regulations evolve with more binding constraints. In general, it is only required to update the allowed energy mix and existing constraints, defining, if needed, new ones expressed in a linear form.

3.1. Problem Formulation

We formulated the optimization problem with the objective function being the overall cost minimization of the energy mix for green H_2 production, as allowed by the European regulations. This mix consists of production from renewable resources, P_{RES}; power purchased from the grid, P_{GRID}; and power purchased from PPAs, P_{PPA}.

$$\min_{x,\delta} J = \Delta T \cdot \sum_{k=1}^{N} [c_{RES}(k)P_{RES}(k) + c_{GRID}(k)P_{GRID}(k) + c_{PPA}(k)P_{PPA}(k)] \quad (1)$$

where $k\ \Delta T$ is the kth time step, N is the number of ΔT in a day, and, $c_{RES}(k)$, $c_{GRID}(k)$, and $c_{PPA}(k)$ represent the cost of excess renewable energy, energy purchased from the grid, and PPAs, respectively, during each ΔT. *The* decision variables in (1) are assumed to be the power from excess renewable energy $P_{RES}(k)$, grid $P_{GRID}(k)$, and PPAs $P_{PPA}(k)$ at the kth ΔT, and they are grouped in x, whereas δ represents binary decision variables $\delta(k)$, defining the time intervals in the day during which the electrolyzer should be turned on.

$$x = [P_{RES},\ P_{GRID}, P_{PPA}] \in \Re \quad \text{and} \quad \delta \in \{0,1\} \quad (2)$$

The following constraints are considered. In detail, (4) limits the renewable energy used for H_2 production by the jth electrolyzer unit to the maximum value $P_{RES}^{max}(k)$ forecasted

in each ΔT. By assuming ΔT equal to 1 h, the power constraints also correspond to the energy constraints.

$$0 \leq P_{RES}(k) \leq P_{RES}^{max}(k) \qquad \forall k \tag{3}$$

$$0 \leq P_{GRID}(k) \leq P_{GRID}^{max}(k) \qquad \forall k \tag{4}$$

$$0 \leq P_{PPA}(k) \leq P_{PPA}^{max}(k) \qquad \forall k \tag{5}$$

Similarly, (5) and (6) limit the required power for H_2 production from the grid and PPAs to the maximum values of $P_{GRID}^{max}(k)$ and $P_{PPA}^{max}(k)$, respectively, forecasted in each ΔT.

Moreover, the electrolyzer unit can operate during a time interval under full-load working conditions, requiring the rated power P_{ETZ}^{rated} for H_2 production, or under partial-load working conditions. Thus, the following constraints are considered. In detail, (6) and (7) impose that the energy mix for the electrolyzer unit be included within the power absorption range according to its load percentage, if it is turned on during a time interval:

$$P_{RES}(k) + P_{GRID}(k) + P_{PPA}(k) \leq Load_{max}\delta_j(k)P_{ETZ}^{rated} \quad \forall k \tag{6}$$

$$P_{RES}(k) + P_{GRID}(k) + P_{PPA}(k) \geq Load_{min}\delta_j(k)P_{ETZ}^{rated} \quad \forall k \tag{7}$$

where $Load_{min}$ and $Load_{max}$ are the minimum- and maximum-load allowable operating conditions for the electrolyzer unit. Of course, by changing the electrolyzer's operating conditions, H_2 production efficiency changes accordingly.

In addition, a maximum number of working hours M for the electrolyzer have also been considered. Constraint (8) considers the aging and cost of the PEM unit, which increase as the working time extends. By limiting the working hours, the electrolyzer is constrained to operate only in the WH_{max} time intervals that minimize the cost of green H_2 production. This constraint is expressed as follows:

$$0 \leq \sum_{k=1}^{N} \delta(k) = WH_{max} \tag{8}$$

Moreover, the maximum amount of energy purchased from the grid, according to the DRA, is limited by (9), where α represents the percentage value of RESs. Similarly, the maximum amount of energy purchased from PPAs, E_{PPA}^{tot}, is limited by (10).

$$0 \leq \Delta T \cdot \sum_{k=1}^{N} P_{GRID}(k) \leq \alpha \cdot \Delta T \cdot \sum_{k=1}^{N} P_{RES}(k) + P_{GRID}(k) + P_{PPA}(k) \tag{9}$$

$$0 \leq \Delta T \cdot \sum_{k=1}^{N} P_{PPA}(k) \leq E_{PPA}^{tot} \tag{10}$$

Finally, the daily target of green H_2 production, denoted as H_2^{target}, is also constrained. The absorbed energy mix must be weighted by the system efficiency to obtain the desired amount of H_2 by the end of the day. The target production of H_2 is established by evaluating the supply contracts stipulated by the owner of the electrolyzer units. Thus, it is necessary to model the electrolyzer system efficiency to properly estimate H_2 production. In this paper, we consider the electrolyzer system efficiency including both the stack and its auxiliary system efficiency (Figure 4). Thus, the electrolyzer system efficiency, η, which depends on the input electrical power, is modeled as a piecewise function, as follows:

$$\eta(P) = \begin{cases} \eta_1 & \forall\, P \geq 0 \ \cap P < P_1 \\ \eta_2 & \forall\, P \geq P_1 \cap P < P_2 \\ \cdots & \\ \eta_M & \forall\, P \geq P_{M-1} \cap P < P_M \end{cases} \tag{11}$$

where η_i represents the ith efficiency value related to the input power value P within the $[P_{i-1}, P_i[$ interval. Moreover, M is the number of different efficiency values in the piecewise function, and P is the sum of P_{RES}, P_{GRID}, and P_{PPA} at the kth time step.

It is also necessary to introduce a binary variable z that is equal to one if and only if the electrolyzer input power P is within its corresponding power interval. For example, if P is within the interval P_{i-1} and P_i, only z_i should take the value of one while other z variables take the value of zero. In this way, only η_i is assumed to be the electrolyzer system efficiency. Consequently, $\eta(P)$ can be expressed as follows:

$$\eta(P) = P\ (\ \eta_1 \cdot z_1 + \ \eta_2 \cdot z_2 + \cdots + \ \eta_M \cdot z_M) \tag{12}$$

where z_i are auxiliary variables defined as $z \in \{0, 1\}$ and subjected to the constraint below.

$$0 \leq \sum_{i=1}^{M} z_i \ \leq 1 \tag{13}$$

Thus, the daily target of green H_2 production, H_2^{target}, is described by the following constraint:

$$H_2^{production} = H_2^{target} \tag{14}$$

where

$$H_2^{production} = \sum_{k=1}^{N} \sum_{j=1}^{M} (P_{RES}(k) + P_{GRID}(k) + P_{PPA}(k)) \cdot z_j \cdot \eta_j \tag{15}$$

In (15), the terms $P_{RES}(k) \cdot z_j$, $P_{GRID}(k) \cdot z_j$, and $P_{PPA}(k) \cdot z_j$ represent the product of a continuous variable by a discrete one. These products introduce a nonlinear component into the problem. However, it can be linearized using the methodology described in Section 3.2.

3.2. Linearization of the H_2 Target Constraint

In the technical literature, several techniques are proposed to model logical components of processes (on/off switches, discrete mechanisms, combinational and sequential networks) and heuristics knowledge about plant operations as mixed-integer linear inequalities, i.e., linear inequalities involving both continuous and logical variables [41]. This approach leads to mixed logical dynamical (MLD) systems described by linear dynamic equations subject to linear mixed-integer inequalities, which involve both continuous and binary variables.

In particular, [41] proposes the following methodology to model $\delta f(x)$, where $f(x) : \Re^n \mapsto \Re$ and $\delta \in \{0, 1\}$. This product can be replaced by an auxiliary real variable $y \triangleq \delta f(x)$, which satisfies $[\delta = 0] \longrightarrow [y = 0]$ and $[\delta = 1] \longrightarrow [y = f(x)]$. In detail, equation $y = \delta f(x)$ is equivalent to the following:

$$\begin{gathered} y \leq Max \cdot \delta \\ y \geq Min \cdot \delta \\ y \leq f(x) - Min \cdot (1 - \delta) \\ y \geq f(x) - Max \cdot (1 - \delta) \end{gathered} \tag{16}$$

where

$$\begin{aligned} Max &\triangleq \max_x f(x) \\ Min &\triangleq \min_x f(x) \end{aligned} \tag{17}$$

According to the above methodology, (15) can be rewritten in the following form by introducing auxiliary variables :

$$H_2^{production} = \sum_{k=1}^{N} \sum_{j=1}^{M} \left(y_{RES,j} + y_{GRID,j} + y_{PPA,j}\right) \cdot \eta_j \tag{18}$$

where $y_{RES,j}$, $y_{GRID,j}$, and $y_{PPA,j}$ are continuous auxiliary variables, defined below.

$$y = [y_{RES},\ y_{GRID}, y_{PPA}] \in \Re \tag{19}$$

Moreover, auxiliary variables $y_{RES,j}$, $y_{GRID,j}$, and $y_{PPA,j}$ are subject to the following constraints:

$$\begin{array}{ll} y_{RES,j}(k) \le P_{RES}^{max}(k) \cdot z_j & \forall k,\ \forall j \\ y_{RES,j}(k) \ge 0 & \forall k,\ \forall j \\ y_{RES,j}(k) \le f(x) & \forall k,\ \forall j \\ y_{RES,j}(k) \ge f(x) - P_{RES}^{max}(k) \cdot (1 - z_j) & \forall k,\ \forall j \end{array} \tag{20}$$

$$\begin{array}{ll} y_{GRID,j}(k) \le P_{GRID}^{max}(k) \cdot z_j & \forall k,\ \forall j \\ y_{GRID,j}(k) \ge 0 & \forall k,\ \forall j \\ y_{GRID,j}(k) \le f(x) & \forall k,\ \forall j \\ y_{GRID,j}(k) \ge f(x) - P_{GRID}^{max}(k) \cdot (1 - z_j) & \forall k,\ \forall j \end{array} \tag{21}$$

$$\begin{array}{ll} y_{PPA,j}(k) \le P_{PPA}^{max}(k) \cdot z_j & \forall k,\ \forall j \\ y_{PPA,j}(k) \ge 0 & \forall k,\ \forall j \\ y_{PPA,j}(k) \le f(x) & \forall k,\ \forall j \\ y_{PPA,j}(k) \ge f(x) - P_{PPA}^{max}(k) \cdot (1 - z_j) & \forall k,\ \forall j \end{array} \tag{22}$$

Finally, the proposed cost optimization problem for scheduling electrolyzer operations is defined by the objective function (1) and constraints (3)–(10), (18), and (20)–(22), where x and y are continuous decision variables, while δ and z are binary decision variables. Thus, the nonlinear problem described in Section 3.1 can be transformed into an MILP problem by replacing the products of discrete and continuous variables with auxiliary continuous variables, allowing it to be efficiently solved using existing commercial tools.

4. Simulation Framework

In this Section, the proposed case study defined in accordance with EU regulations is introduced. Additionally, several scenarios are evaluated using seasonal data, and a representative set of simulation results is presented and discussed.

4.1. Case Study

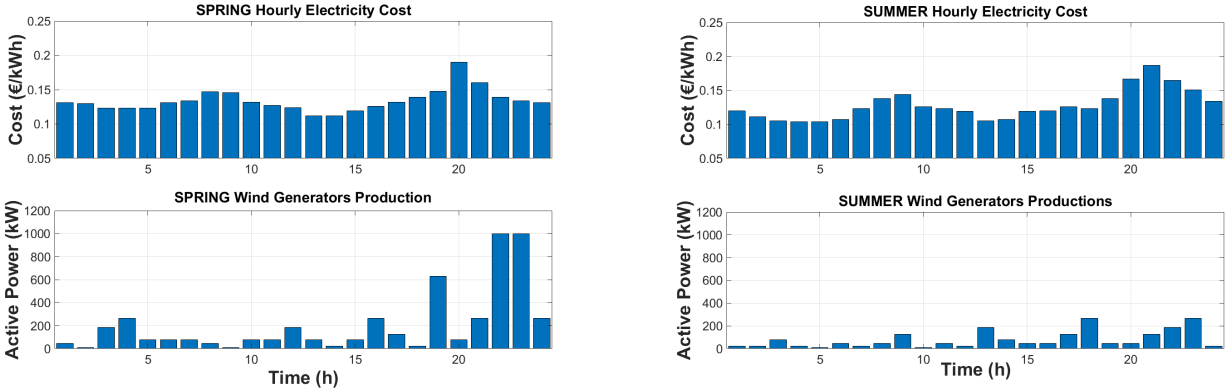
A green H_2 production plant consisting of a 1 MW PEM electrolyzer has been considered. As reported in Section 2.1, PEM technologies are becoming the most widespread and allow for a rapid electrolyzer response to changes in RES availability, making ramp-up and ramp-down time intervals neglectable. It is also assumed that the minimum allowed load for the electrolyzer is equal to 40% of its full power, and the electrolyzer system efficiency, modeled as a piecewise function, has been split in M = 5 equal parts. In this way, the efficiency value changes if the electrolyzer load varies by more than 20% of its rated power. The electrolyzer efficiency at full load is assumed to be 20 kg/MW, whereas the efficiency peak value is assumed to be 22.2 kg/MW.

A group of wind power generators sharing the same total rated power of the electrolyzer is also installed in the plant. The cost of the wind power locally produced is assumed to be constant and equal to 0.05 EUR/kWh. The produced H_2 can only be transported to end-users because it is assumed that there is no H_2 storage on-site and/or fuel cells to reconvert H_2 into electricity. According to the EU regulatory framework, the energy required for the H_2 production plant can also be obtained from the grid and/or from PPAs. It is assumed that the plant is in a bidding zone with an average renewable electricity share exceeding 90% in the previous calendar year, allowing for the purchase energy from the grid in relation to the proportion of renewable electricity in the bidding zone.

Therefore, assuming the green H_2 production plant to be located in the south of Italy, the average share of RES is about 17% (α = 0.17). Thus, the total amount of energy allowed from the grid is set to be 17% of the energy required to reach the target production of green

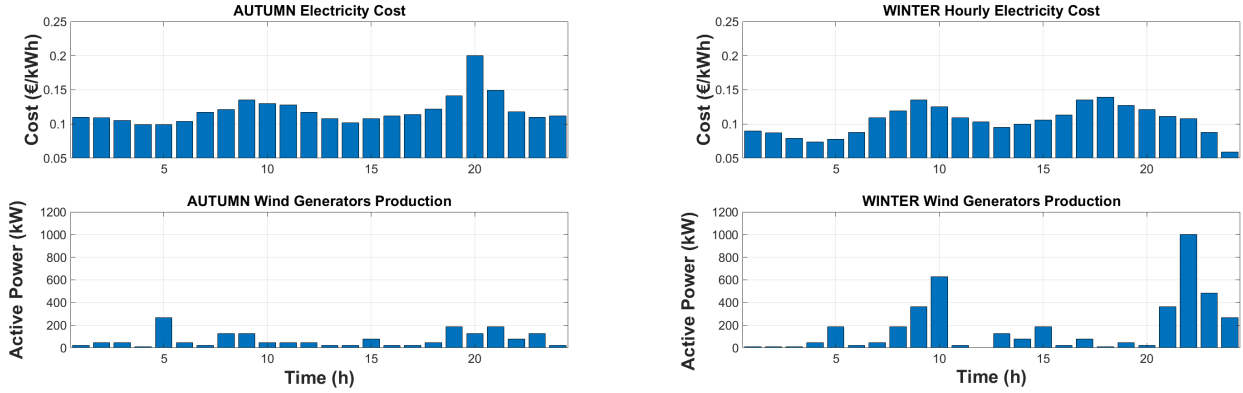
H_2. Finally, the cost for the PPAs is assumed to be constant during the day and equal to 0.15 EUR/kWh.

The green H_2 target production is set to 240 kg/day requiring electrical energy equal to 12 MWh/day, assuming that the electrolyzer is working at full power. In this scenario, the maximum number of electrolyzer working hours is $\delta = 12$. Thus, the daily maximum energy that can be purchased from the grid is about 2 MWh. Figures 5 and 6 depict the forecasted hourly power production of the RES on site [42], and the hourly electricity cost for energy purchased from the grid, according to data provided by the Italian Power Exchange [43]. Four typical days for each season have been selected. Finally, the obtained results are compared with the average production cost of gray H_2 in 2023, produced from natural gas without abatement, which is equal to 1.96 EUR/kg, and that of blue H_2, i.e., produced from natural gas with carbon capture, equal to 2.85 EUR/kg [44].



(**a**) (**b**)

Figure 5. Daily electricity cost and RES production for (**a**) a typical spring day and (**b**) a typical summer day.



(**a**) (**b**)

Figure 6. Daily electricity cost and RES production for (**a**) a typical autumn day and (**b**) a typical winter day.

4.2. Numerical Results

Here, a representative set of the results obtained from numerical simulations is presented. The Global Optimization Toolbox of MATLAB is employed to solve the proposed MILP problem. Several scenarios considering different H_2 daily production targets, RES generation, and costs for PPAs are described, as follows:

- Scenario 1—case study;
- Scenario 2—25% reduction in H_2 production target;
- Scenario 3—25% increase in H_2 production target;

- Scenario 4—50% reduction in RES production;
- Scenario 5—reduced PPA cost to 0.10 EUR/kWh.

The following figures refer to scenario 1, comparing the ON-OFF operating strategy with the PARTIAL-LOAD strategy. In detail, the optimal energy mix and compliance with constraints for green H_2 production are shown in Figures 7–14, considering different seasons. The time intervals during which the electrolyzers must be turned ON, along with the energy absorbed by on-site wind generators from the grid and PPAs, are presented from top to bottom in Figures 7, 9, 11 and 13, respectively. The daily forecasted production by RES is highlighted with a red line. In scenario 1, H_2 production takes 12 h to reach the daily target; thus, the algorithm minimizes the production cost by turning ON the electrolyzers in time intervals during which the use of on-site RESs is maximized according to the additionality criterion. Energy from the grid and PPAs contribute to the energy mix, according to their hourly cost, to minimize the total energy cost.

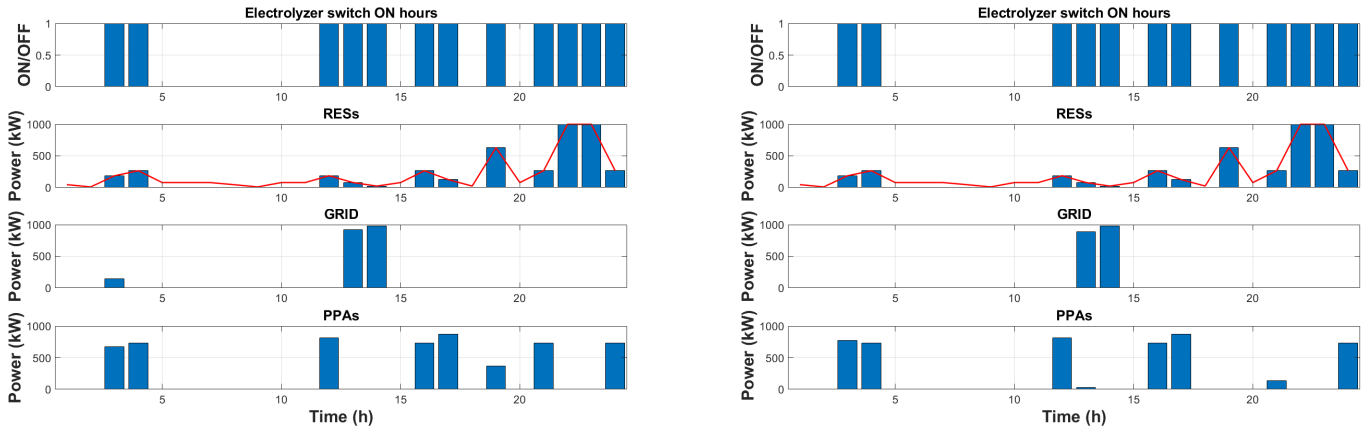


Figure 7. Scenario 1, assuming SPRING data and δ = 12: (**a**) energy mix according to the ON/OFF operating strategy; and (**b**) energy mix according to the PARTIAL-LOAD operating strategy.

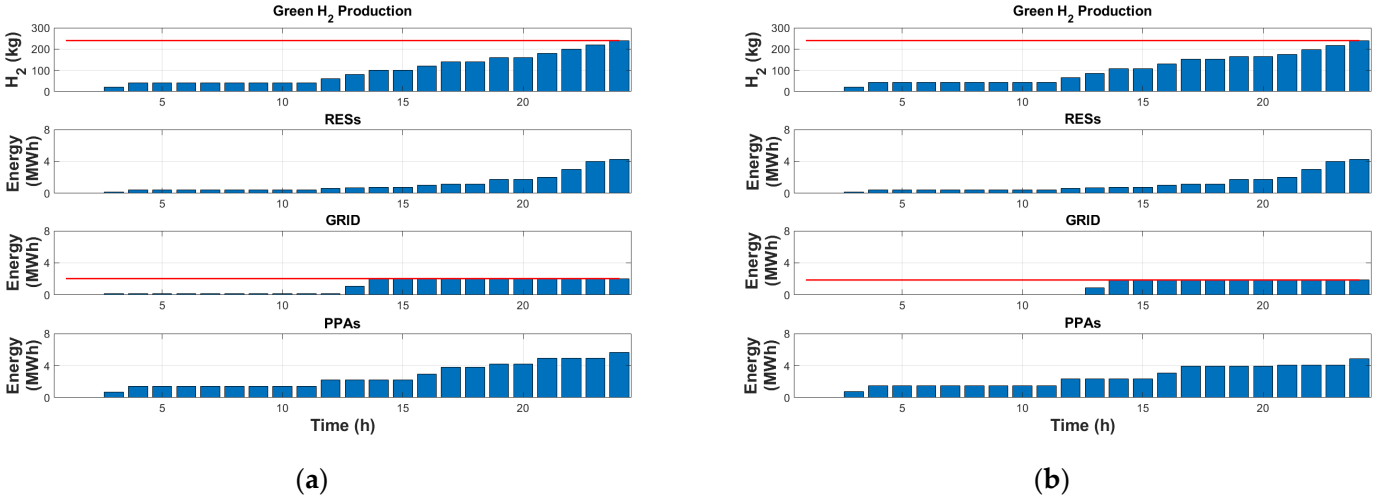
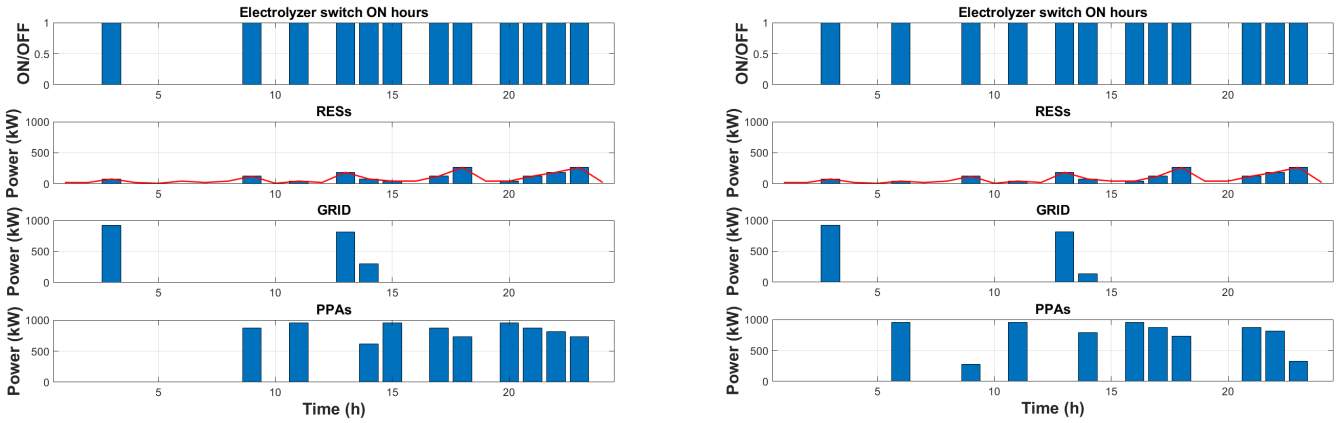
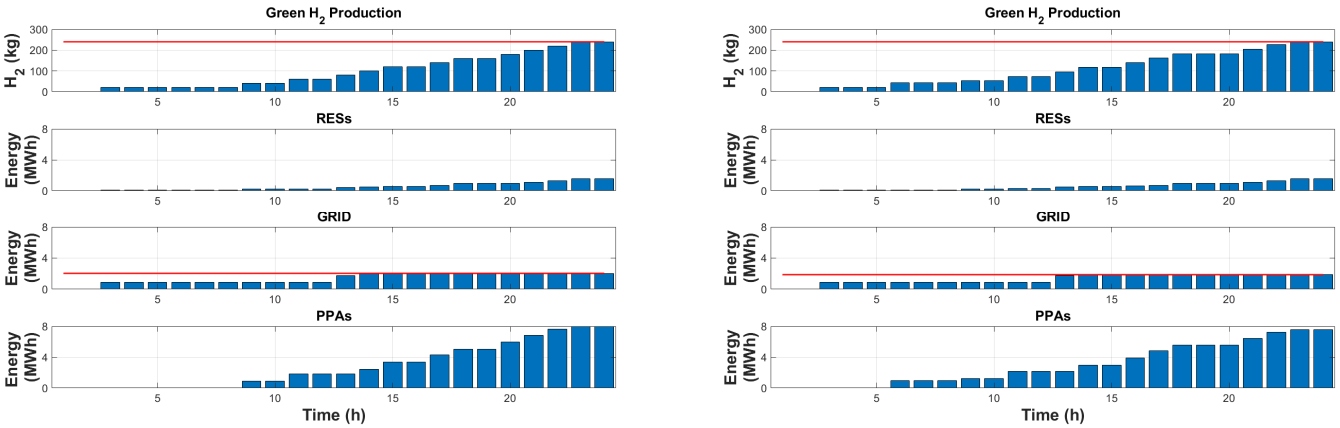


Figure 8. Scenario 1, assuming SPRING data and δ = 12: (**a**) H_2 production constraints assuming the ON/OFF operating strategy; and (**b**) H_2 production constraints assuming the PARTIAL-LOAD operating strategy.



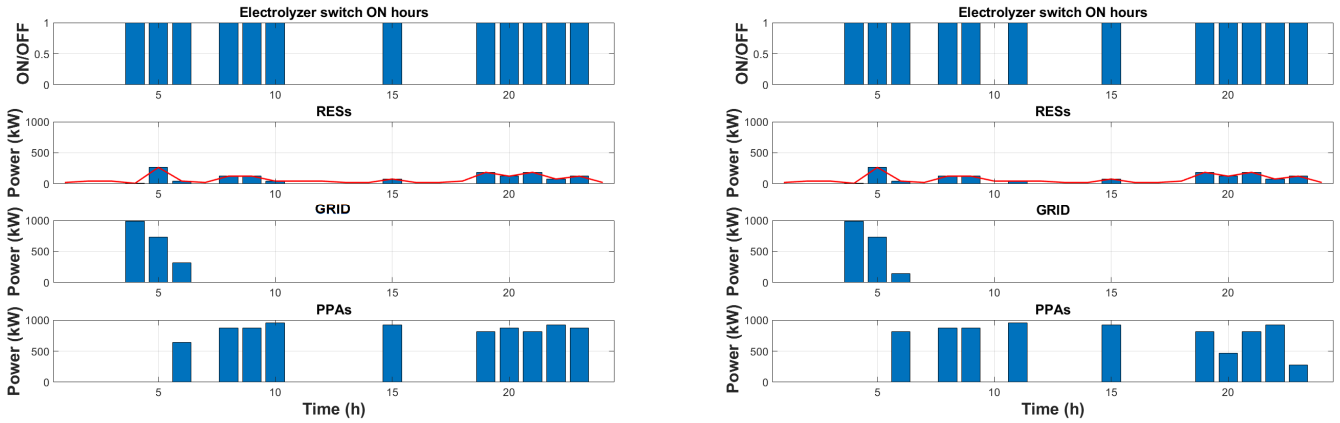
(**a**) (**b**)

Figure 9. Scenario 1, assuming SUMMER data and δ = 12: (**a**) energy mix according to the ON/OFF operating strategy; and (**b**) energy mix according to the PARTIAL-LOAD operating strategy.



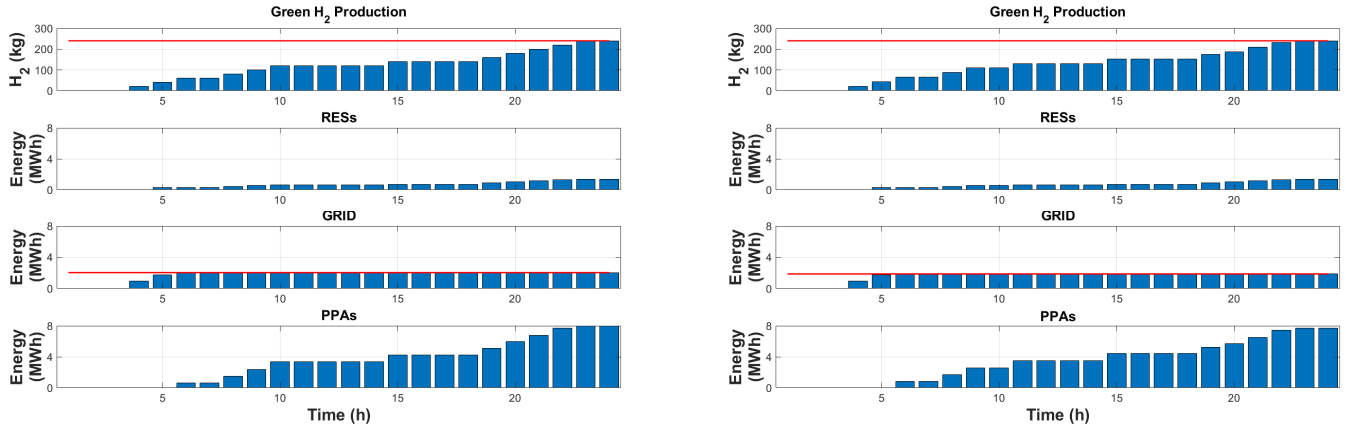
(**a**) (**b**)

Figure 10. Scenario 1, assuming SUMMER data and δ = 12: (**a**) H_2 production constraints assuming the ON/OFF operating strategy; and (**b**) H_2 production constraints assuming the PARTIAL-LOAD operating strategy.



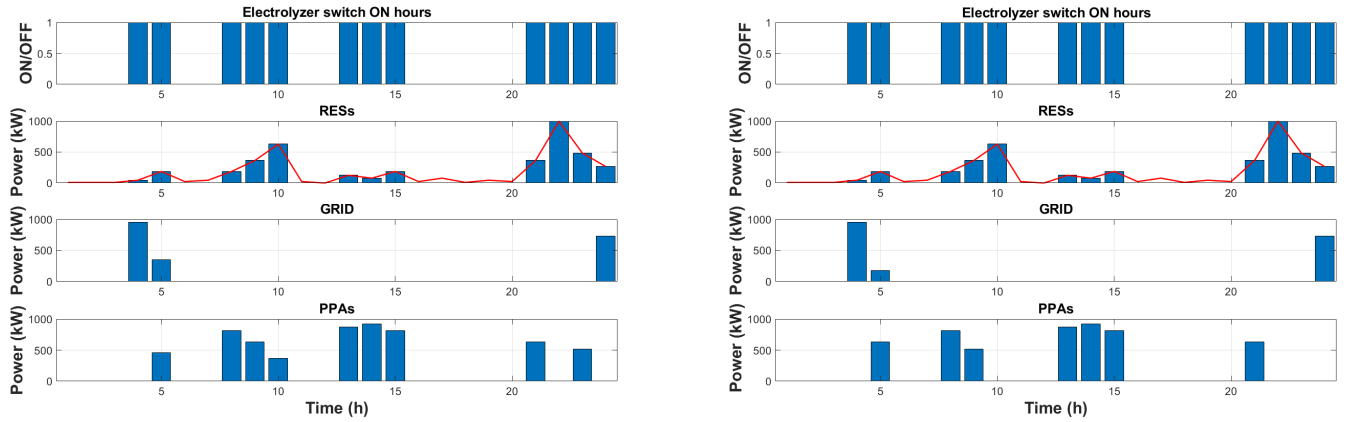
(**a**) (**b**)

Figure 11. Scenario 1, assuming AUTUMN data and δ = 12: (**a**) energy mix according to the ON/OFF operating strategy; and (**b**) energy mix according to the PARTIAL-LOAD operating strategy.



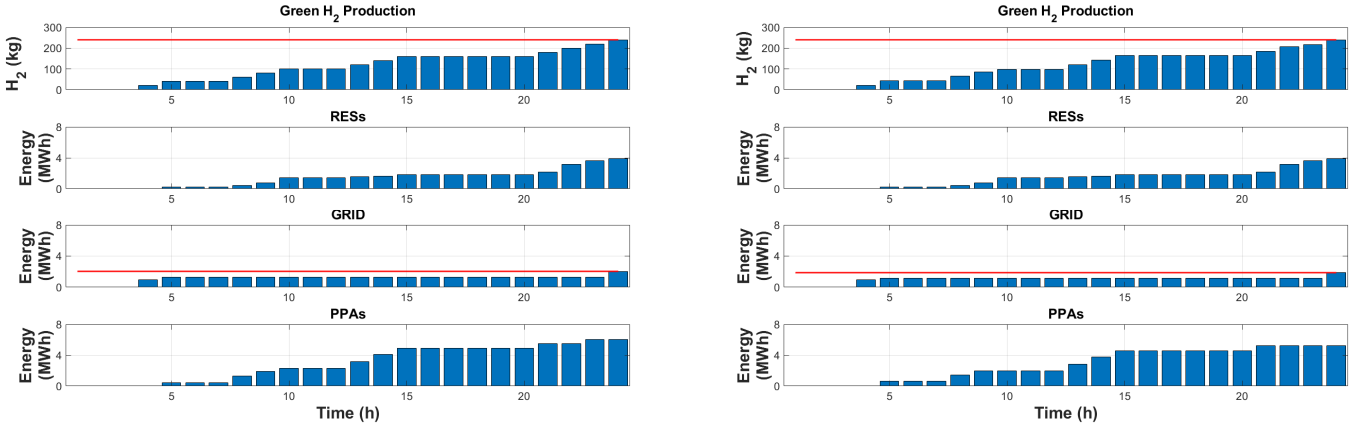
(**a**) (**b**)

Figure 12. Scenario 1, assuming AUTUMN data and δ = 12: (**a**) H_2 production constraints assuming the ON/OFF operating strategy; and (**b**) H_2 production constraints assuming the PARTIAL-LOAD operating strategy.



(**a**) (**b**)

Figure 13. Scenario 1, assuming WINTER data and δ = 12: (**a**) energy mix according to the ON/OFF operating strategy; and (**b**) energy mix according to the PARTIAL-LOAD operating strategy.



(**a**) (**b**)

Figure 14. Scenario 1, assuming WINTER data and δ = 12: (**a**) H_2 production constraints assuming the ON/OFF operating strategy; and (**b**) H_2 production constraints assuming the PARTIAL-LOAD operating strategy.

The constraints imposed on the daily production target of green H_2 and the limit of daily energy taken from the grid are met in scenario 1 for each season, and they are shown in Figures 8, 10, 12 and 14. The daily targets/limits are highlighted with a red line, while the bars indicate the cumulated energy over time. In this scenario, if the energy purchased from the grid reaches the maximum value imposed by the EU regulations and there is not enough energy from on-site RES, then the plant owner has no choice but to purchase energy via PPAs assumed to have a higher cost.

Tables 1–3 present a synthetic comparison among the proposed scenarios, using spring data to highlight the effect of the energy mix on the production cost of green H_2. In detail, energy purchased from the grid in scenarios 2–3 is different according to the EU regulations, and it depends on the H_2 production target. Then, scenario 2 demonstrates a lower H_2 production cost than scenario 1 because, if the required energy is reduced, it allows for the use of a lower-cost energy mix. Conversely, scenario 3 shows a higher production cost. The daily target production is different, and, to meet this constraint, a different energy mix with varying costs is required.

Table 1. Scenario comparison assuming SPRING data: ON-OFF scheduling strategy.

Scenarios	E_{RES} (MWh)	E_{GRID} (MWh)	E_{PPA} (MWh)	H_2 Cost (EUR/kg)	Increase in H_2 Cost (%)
Gray H_2	-	-	-	1.96, [20]	-
Blue H_2	-	-	-	2.85, [20]	45
#1	4.29	2.04	5.67	5.39	175
#2	4.06	1.43	3.40	5.01	156
#3	4.53	2.55	7.92	5.68	189
#4	2.15	2.04	7.81	6.28	220
#5	4.35	0	7.65	4.09	109

Table 2. Scenario comparison assuming SPRING data: partial-load scheduling strategy (electrolyzer working hours $\leq$ 2).

Scenarios	E_{RES} (MWh)	E_{GRID} (MWh)	E_{PPA} (MWh)	H_2 Cost (EUR/kg)	Increase in H_2 Cost (%)
Gray H_2	-	-	-	1.96, [20]	-
Blue H_2	-	-	-	2.85, [20]	45
#1	4.29	1.87	4.83	4.78	143
#2	4.35	1.40	2.49	4.18	113
#3	-	-	-	-	-
#4	2.15	1.87	6.98	5.68	190
#5	4.35	0	6.64	3.67	87

Table 3. Scenario comparison assuming SPRING data: partial-load scheduling strategy (electrolyzer working hours $\leq$ 18).

Scenarios	E_{RES} (MWh)	E_{GRID} (MWh)	E_{PPA} (MWh)	H_2 Cost (EUR/kg)	Increase in H_2 Cost (%)
Gray H_2	-	-	-	1.96, [20]	-
Blue H_2	-	-	-	2.85, [20]	45
#1	4.76	1.87	4.36	4.59	134
#2	4.74	1.40	2.10	3.99	103
#3	4.76	2.33	6.64	4.99	154
#4	2.38	1.87	6.74	5.58	185
#5	4.82	0	6.17	3.57	82

In scenario 3, the electrolyzer's operating hours increase, necessitating the purchase of more energy via PPAs, which are assumed to have higher costs compared to on-site RES

and grid energy. In scenario 4, a reduction of 50% in RES production is assumed, resulting in an increased reliance on energy from PPAs, significantly impacting the H_2 production cost, which is the highest among the considered scenarios. Finally, scenario 5 illustrates the effect of a reduced cost of PPAs (about 33%). However, the grid contribution to the energy mix does not increase due to the average lower cost of grid electricity.

Specifically, Table 1 presents the energy mix and H_2 production costs, assuming the ON-OFF strategy. Table 2 provides similar information, assuming the PARTIAL-LOAD strategy with $\delta \leq 12$. In Table 3, the PARTIAL-LOAD strategy with $\delta \leq 18$ is considered.

It is worth noting that the WH_{max} value for the ON-OFF strategy changes according to the daily target for green H_2. By imposing the full-power operating condition and considering the production rate in these operating conditions, the working hours are straightforward to derive. For the PARTIAL-LOAD strategy, instead, the WH_{max} value is imposed and does not change. In such a way, some scenarios could not be feasible, e.g., scenario 3 in Table 2. Indeed, in such a scenario, WH_{max} is equal to 12, whereas the minimum feasible value is 15, as computed in Table 1.

The advantage of using the PARTIAL-LOAD strategy over the ON-OFF strategy is especially highlighted when the number of electrolyzer operating hours is huge. As the maximum number of the electrolyzer working hours increases, a small reduction in H_2 cost can be achieved, as it can utilize more time slots to optimize production costs. However, the electrolyzer operates at partial-load conditions for a longer duration, which incurs additional costs, tending to increase, that need to be considered in the estimated H_2 production cost. This aspect is not the focus of this paper, due to the need to model electrolyzer aging and degradation costs according to the operating conditions, but it will be addressed in a future study.

5. Conclusions

In 2023, the European Commission formally published the two delegated acts outlining detailed rules on the EU definition of green hydrogen. This paper presents a methodology for planning the operation of electrolyzers located near RES power plants, aimed at minimizing the cost of green electrical energy to meet the target H_2 production under the EU regulations.

The cost optimization problem has been formulated as an MILP problem, and the nonlinear constraint related to the daily target of green H_2 production has been modeled as linear inequalities involving both continuous and logical variables. Moreover, electrolyzer efficiency has been included in the mathematical formulation as a piecewise function, and constraints on the energy mix imposed by the current regulatory framework have also been modeled.

Simulation results considering different scenarios are presented and discussed. However, comparing the obtained results with those presented in previous studies can lead to conclusions that are difficult to generalize. Then, it is shown that the obtained estimations are consistent with actual market trends of green H_2 production costs. Indeed, [44] reports an average production cost in 2023 of 5.89 EUR/kg for green H_2, whereas the results obtained in this paper show an average cost among the scenarios of 5.29 EUR/kg, assuming the ON-OFF strategy, which could be reduced to 4.54 EUR/kg assuming the PARTIAL-LOAD strategy. A limitation of the proposed model is that these costs reflect only the production expenses related to the energy mix and do not account for other costs such as electrolyzer operation and maintenance (O&M) and depreciation. As a general consideration, even with an optimized energy mix, green H_2 remains more expensive than gray and blue H_2 (+170% and +125%, respectively, assuming an ON-OFF strategy). Although the proposed simulations show a green H_2 cost per kg comparable to data in [44], the green H_2 cost in each scenario is still higher than that of gray and blue H_2. A significant reduction in the price of green H_2 cannot be achieved without applying economies of scale and supportive policies.

Future research directions include the modeling of electrolyzer aging and degradation costs according to the operating conditions to perform techno-economic analysis also considering electrolyzer installation and O&M costs. Moreover, the optimal sizing and operation of a green H_2 production plant consisting of more electrolyzers, H_2 storage, and fuel cells for producing electricity can be approached starting from this work. Finally, the effect of uncertainty related to electricity costs and RES production, extreme weather conditions, and/or grid outages on the production cost of green H_2 can significantly extend the results obtained in this paper.

Author Contributions: Conceptualization, G.G. and V.C.; methodology, G.G., V.C. and A.V.; software, G.G. and F.D.C.; validation, G.G., V.C. and F.D.C.; formal analysis, G.G. and A.V.; investigation, G.G. and F.D.C.; resources, G.G., V.C. and V.G.; data curation, G.G. and V.C.; writing—original draft preparation, G:G. and F.D.C.; writing—review and editing, V.C., V.G., G.G. and L.I.; visualization, G.G. and V.C.; supervision, A.V., V.G. and L.I.; project administration, V.G.; and funding acquisition, V.G. All authors have read and agreed to the published version of the manuscript.

Funding: This research received no external funding.

Data Availability Statement: The raw data supporting the conclusions of this article will be made available by the authors upon request.

Conflicts of Interest: The authors declare no conflicts of interest.

References

1. Renewable Power-to-Hydrogen—Innovation Landscape Brief—International Renewable Energy Agency (IRENA). 2019. Available online: https://www.irena.org/-/media/Files/IRENA/Agency/Publication/2019/Sep/IRENA_Power-to-Hydrogen_Innovation_2019.pdf (accessed on 21 September 2024).
2. The Future of Hydrogen Seizing Today's Opportunities—International Energy Agency (IEA). 2019. Available online: https://www.iea.org/reports/the-future-of-hydrogen (accessed on 21 September 2024).
3. Renewable Energy Directive—European Commission (EU). 2023. Available online: https://energy.ec.europa.eu/topics/renewable-energy/renewable-energy-directive-targets-and-rules/renewable-energy-directive_en (accessed on 21 September 2024).
4. EU Rules for Renewable Hydrogen—European Parliament. 2023. Available online: https://www.europarl.europa.eu/RegData/etudes/BRIE/2023/747085/EPRS_BRI(2023)747085_EN.pdf (accessed on 21 September 2024).
5. Ennassiri, Y.; Belhaj, I.; Bouzekri, H. Techno-Economic Assessment of Hydrogen Production from vRE in Morocco Case Study: Laayoune, Ouarzazate, Midelt. In Proceedings of the 7th International Renewable and Sustainable Energy Conference, Agadir, Morocco, 27–30 November 2019.
6. Papadopoulos, V.; Knockaert, J.; Develder, C.; Desmet, J. Techno-economic study of hydrogen production using PV, wind power and battery storage. In Proceedings of the IEEE PES Innovative Smart Grid Technologies Europe, Bucharest, Romania, 29 September–2 October 2019.
7. Mendler, F.; Garcia, J.F.; Voglstätter, C. Global optimization of capacity ratios between electrolyser and renewable electricity source to minimize levelized cost of green hydrogen. *Int. J. Hydrogen Energy* **2024**, *82*, 986–993. [CrossRef]
8. Farah, S.; Bokde, N.; Andresen, G.B. Cost and CO_2 emissions co-optimisation of green hydrogen production in a grid-connected renewable energy system. *Int. J. Hydrogen Energy* **2024**, *84*, 164–176. [CrossRef]
9. Hussam, W.K.; Barhoumi, E.M.; Abdul-Niby, M.; Sheard, G.J. Techno-economic analysis and optimization of hydrogen production from renewable hybrid energy systems: Shagaya renewable power plant-Kuwait. *Int. J. Hydrogen Energy* **2024**, *58*, 56–68. [CrossRef]
10. Halloran, C.; Leonard, A.; Salmon, N.; Müller, L.; Hirmer, S. GeoH2 model: Geospatial cost optimization of green hydrogen production including storage and transportation. *MethodsX* **2024**, *12*, 102660. [CrossRef]
11. Jodry, A.; Girard, R.; Nóbrega, P.H.A.; Molinier, R.; Faris, M.D.E.A. Hydrogen production via electrolysis in 2030: Comparing four connection schemes through energy system optimization. In Proceedings of the IEEE PES Innovative Smart Grid Technologies Europe, Grenoble, France, 23–26 October 2023.
12. Ren, Y.; Jin, K.; Gong, C.; Hu, J.; Liu, D.; Jing, X.; Zhang, K. Modelling and capacity allocation optimization of a combined pumped storage/wind/photovoltaic/hydrogen production system based on the consumption of surplus wind and photovoltaics and reduction of hydrogen production cost. *Energy Convers. Manag.* **2023**, *296*, 117662. [CrossRef]
13. Jiang, S.; Huang, H.; Chi, B.; Cao, X.; Shu, N.; Fan, F. Topology and Configuration Optimization of Wind-Solar-Hydrogen Combined System. In Proceedings of the IEEE/IAS Industrial and Commercial Power System Asia, Chongqing, China, 7–9 July 2023.
14. Feng, C.; Shao, C.; Xiao, Y.; Dong, Z.; Wang, X. Day-Ahead Strategic Operation of Hydrogen Energy Service Providers. *IEEE Trans. Smart Grid Year* **2022**, *13*, 3493–3507. [CrossRef]
15. Kookos, I.K. Systematic optimization of off-grid green hydrogen production systems. *Int. J. Hydrogen Energy* **2024**, *79*, 1299–1312. [CrossRef]

16. Pan, J.; Lei, J.; Chen, A.; Cao, Y.; Zhao, Z.; Zhang, H. Optimal Proportion of Wind, PV, Hydrogen and Storage Capacity Based on Time Sequence Simulation. In Proceedings of the 5th International Conference on Power and Energy Applications, Guangzhou, China, 18–20 November 2022.
17. Chen, Z.; Yu, L.; Zhang, D.; Jiang, Q. Smart Operation Optimization Methods for Hydrogen-Based Energy Systems Under Uncertainties. In Proceedings of the China Automation Congress, Chongqing, China, 17–19 November 2023.
18. Li, Y.; Wen, F.; Tian, F.; Xue, Y.; Dong, Z.; Zheng, Y.; Zhang, R. Day-ahead schedule of a multi-energy system with power-to-gas technology. In Proceedings of the IEEE Power & Energy Society General Meeting, Chicago, IL, USA, 16–20 July 2017.
19. Chen, Z.; Zhang, Y.; Su, J. Optimal capacity configuration for power to gas facilities in a wind farm: A bi-level programming. In Proceedings of the International Conference on Power System Technology, Guangzhou, China, 6–9 November 2018.
20. Gu, Z.; Pan, G.; Gu, W.; Qiu, H.; Lu, S. Robust Optimization of Scale and Revenue for Integrated Power-to-Hydrogen Systems Within Energy, Ancillary Services, and Hydrogen Markets. *IEEE Trans. Power Syst.* **2023**, *39*, 5008–5023. [CrossRef]
21. Pirom, W.; Srisiriwat, A. Experimental Study of Hybrid Photovoltaic-PEM Electrolyzer-PEM Fuel Cell System. In Proceedings of the International Electrical Engineering Congress, Khon Kaen, Thailand, 9–11 March 2022.
22. Barhoumi, E.M.; Okonkwo, P.C.; Zghaibeh, M.; Belgacem, I.B.; Farhani, S.; Bacha, F. Optimization of PV-Grid Connected System Based Hydrogen Refueling Station. In Proceedings of the 8th International Conference on Control, Decision and Information Technologies, Istanbul, Turkey, 17–20 May 2022.
23. Wang, J.; Wen, J.; Wang, J.; Yang, B.; Jiang, L. Coordinated scheduling of wind-solar-hydrogen-battery storage system for techno-economic-environmental optimization of hydrogen production. *Energy Convers. Manag.* **2024**, *314*, 118695. [CrossRef]
24. Ghosh, S.; Jain, R.; Veda, S.; Terlip, D. Improving Distribution System Operations Using Fleet Control of Electrolyzers. In Proceedings of the IEEE/PES Transmission and Distribution Conference and Exposition, Chicago, IL, USA, 12–15 October 2020.
25. Scolaro, M.; Kittner, N. Optimizing hybrid offshore wind farms for cost-competitive hydrogen production in Germany. *Int. J. Hydrogen Energy* **2022**, *47*, 6478–6493. [CrossRef]
26. Shangguan, Z.; Li, H.; Yang, B.; Zhao, Z.; Wang, T.; Jin, L.; Zhang, C. Optimization of alkaline electrolyzer operation in renewable energy power systems: A universal modeling approach for enhanced hydrogen production efficiency and cost-effectiveness. *Int. J. Hydrogen Energy* **2024**, *49*, 943–954. [CrossRef]
27. Li, W.; Zou, Y.; Yang, H.; Fu, X.; Xiang, S.; Li, Z. Two stage Stochastic Energy Scheduling for Multi Energy Rural Microgrids with Irrigation Systems and Biomass Fermentation. *IEEE Trans. Smart Grid* **2024**, 1–12. [CrossRef]
28. Sun, X.; Cao, X.; Zeng, B.; Zhai, Q.; Başar, T.; Guan, X. Stochastic-Robust Planning of Networked Hydrogen-Electrical Microgrids: A Study on Induced Refueling Demand. *IEEE Trans. Smart Grid* **2024**, 1–16. [CrossRef]
29. Ren, Z.; Li, H.; Sun, Z.; Feng, J.; Xia, W. A multi-stage stochastic dispatching method for electricity-hydrogen integrated energy systems driven by model and data. *Appl. Energy* **2024**, *371*, 123668.
30. PEM Electrolyser Technology Flexible, Efficient and Scalable—Siemens Energy. 2021. Available online: https://energyforum.in/fileadmin/india/media_elements/Presentations/20210714_h2_large/Siemens_Energy.pdf (accessed on 21 September 2024).
31. Shiva Kumar, S.; Lim, H. An overview of water electrolysis technologies for green hydrogen production. *Elsevier Energy Rep.* **2022**, *8*, 13793–13813. [CrossRef]
32. Ghadim, H.V.; Canessa, R.; Haas, J.; Peer, R. Electrolyzer cost projections compared to actual market costs: A Critical Analysis. In Proceedings of the IEEE PES Innovative Smart Grid Technologies, Auckland, New Zealand, 21–24 November 2023.
33. Sapountzi, F.M.; Gracia, J.M.; Weststrate, C.J.; Fredriksson, H.O.A.; Niemantsverdriet, J.W. Electrocatalysts for the generation of hydrogen, oxygen and synthesis gas. *Prog. Energy Combust. Sci.* **2017**, *58*, 1–35. [CrossRef]
34. Gürbüz, H.; Akçay, H.; Akçay, I.H.; Demirtürk, S. Experimental Study on Operating Characteristics of On-Board PEMe Hydrogen Generator Integrated with a SI Engine. *J. Energy Eng.* **2018**, *144*, 04018055. [CrossRef]
35. Zhao, P.; Wang, J.; Xia, H.; He, W. A novel industrial magnetically enhanced hydrogen production electrolyzer and effect of magnetic field configuration. *Appl. Energy* **2024**, *367*, 123402. [CrossRef]
36. Bespalko, S.; Mizeraczyk, J. Overview of the Hydrogen Production by Plasma-Driven Solution Electrolysis. *Energies* **2022**, *15*, 7508. [CrossRef]
37. PEM Fuel Cell Materials Market Growth Driven by Transportation Sector—IDTechEx. 2024. Available online: https://www.idtechex.com/en/research-article/pem-fuel-cell-materials-market-growth-driven-by-transportation-sector/30582#:~:text=The%20PEM%20fuel%20cell%20for,components%20used%20in%20fuel%20cells (accessed on 21 September 2024).
38. Overview of the PEM Silyzer Family—Siemens Energy. 2020. Available online: https://4echile.cl/wp-content/uploads/2020/10/20200930-SE-NEB-PEM-Electrolyzer-and-Applications_EW.pdf (accessed on 21 September 2024).
39. Comparison of Fuel Cell Technologies—US Departmentof Energy (DOE). 2016. Available online: https://www.energy.gov/eere/fuelcells/articles/comparison-fuel-cell-technologies-fact-sheet (accessed on 2 November 2024).
40. Efficiency—Electrolysis (White Paper)—Siemens Energy. 2021. Available online: https://assets.siemens-energy.com/siemens/assets/api/uuid:5342163d-2333-4c8d-ae85-2a0e8d45db56/white-paper-efficiency-en.pdf (accessed on 21 September 2024).
41. Bemporad, A.; Morari, M. Control of systems integrating logic, dynamics, and constraints. *Automatica* **1999**, *35*, 407–427. [CrossRef]
42. Finamore, A.R.; Calderaro, V.; Galdi, V.; Graber, G.; Ippolito, L.; Conio, G. Improving Wind Power Generation Forecasts: A Hybrid ANN-Clustering-PSO Approach. *Energies* **2023**, *16*, 7522. [CrossRef]

43. MGP—Results—Zonal Prices—Italian Power Exchange. 2023. Available online: https://www.mercatoelettrico.org/en-us/Home/Results/Electricity/MGP/Results/ZonalPrices#IntestazioneGrafico (accessed on 2 November 2024).
44. Green Hydrogen to Undercut Gray Sibling by End of Decade—BloombergNEF. 2023. Available online: https://about.bnef.com/blog/green-hydrogen-to-undercut-gray-sibling-by-end-of-decade/ (accessed on 21 September 2024).

Disclaimer/Publisher's Note: The statements, opinions and data contained in all publications are solely those of the individual author(s) and contributor(s) and not of MDPI and/or the editor(s). MDPI and/or the editor(s) disclaim responsibility for any injury to people or property resulting from any ideas, methods, instructions or products referred to in the content.